Deep Transferable Intelligence for Spatial Variability Characterization and Data-efficient Learning in Biomechanical Measurement

Kiirthanaa Gangadharan, Qingxue Zhang*, *Senior Member, IEEE*

***Abstract*—Biomechanical measurement is of promising value for rehabilitation, assisted-living, and lifestyle management applications. Nevertheless, the understanding is still limited on the spatial variability of biomechanical dynamics that is essential for optimal motion sensor configuration. Besides, training physical activity detectors is usually data-heavy and time-consuming. Targeting these two challenges, in this study, we propose a novel deep transfer intelligence framework, which leverages deep learning to characterize spatial variability of different motion sensors on diverse body locations, and further leverages inter-subject transfer learning to maximize data-efficiency in challenging scarce data learning. More specifically, to characterize the spatial variability, we propose deep convolutional neural networks to investigate capabilities of both different sensor locations and channels, on physical activity measurement. The characterization determines both optimal sensor configuration and optimal channel configuration. Further, we propose a transfer learning approach to mine inter-subject similarity and then share learned knowledge among subjects, thereby minimizing the training effort and maximizing the data-efficiency in the wearable scarce data learning scenario. Our evaluation experiments have determined the optimal sensor location from seven options as thigh, and the optimal sensor&channel configuration from 42 options as thigh-accelerometer-axis-Y. Our experiments have further demonstrated that, with transfer learning under the optimal sensor&channel configuration, only 10% of data from the target subject for model fine-tuning can yield a physical activity detection accuracy up to 91.6%, with a performance boosting of 9% compared with direct learning without transfer learning. Therefore, the deep transferable learning framework will greatly advance spatial variability characterization for optimal sensor and channel configuration, and efficient scarce data learning in biomedical measurement.**

***Index Terms*—Deep Learning, Transfer Learning, Biomedical Instrumentation, Biomechanical Measurement.**

This work was supported in part by the USA NSF CAREER Award Grant 2047849. Any opinions, findings, and conclusions or recommendations expressed in this material are those of the author(s) and do not necessarily reflect the views of the NSF.

K. Gangadharan is with Department of Electrical and Engineering, Purdue University School of Engineering and Technology, IN, USA.

*Q. Zhang is with both Department of Biomedical Engineering, and Department of Electrical and Computer Engineering, Purdue University School of Engineering and Technology, IN, USA. (e-mail: qxzhang@purdue.edu).

I. Introduction

BIOMECHANICAL measurement is of promising value for rehabilitation, assisted-living, and lifestyle management applications. Biomechanical data carries musculoskeletal dynamics, which further relate to other health concerns like the neurological movement disorders. The prevalence of mobility difficulties and/or disabilities, according to Centers for Disease Control and Prevention (CDC) in United States, is impacting one in seven adults, and with age, it increases to two in five adults [1]. Its impacts on children are also reported to be significantly increasing [2].

The biomechanical dynamics measurement, therefore, is attracting intensive interests nowadays [3]. For instance, Panahandeh *et al.* [4] developed an activity measurement system with an inertial measurement unit (IMU) placed on the chest. Lee *et al.* reported an arm motion measurement system with a wearable wireless sensor network. Zou *et al.* [5] developed a system for inertial measurement with sensors placed on the elbow. Liu *et al.* [6] developed a gait measurement system for force monitoring on crutches, for rehabilitation and assistive living purposes. Ashry *et al.* [7] developed a system with a wrist IMU and deep neural network for physical activity recognition.

However, in light of the fact that human biomechanical dynamics are highly different in different body locations [8-10], the understanding of spatial variability of the motion sensors is still limited. The characterization of spatial variability of different sensor locations is essential to determine the optimal sensor configuration strategies, for achieving high robustness and high usability of the biomechanical measurement system. This is the first challenge that we target in this study, aiming to provide comprehensive characterization of the spatial variability of different sensor placement locations, and also to characterize the sensor channels for each sensor location.

Further, the computational models for biomechanical data analytics have also been reported including both non-machine learning and machine learning methods. Panahandeh *et al.* [4] developed a Hidden Markov Model for pedestrian activity classification. Li *et al.* [11] proposed a Kalman filtering method for body motion measurement. Ahmed *et al.* [12] also reported a Kalman method for body orientation estimation. Ashry *et al.* [7] designed a Long Short-Term Memory model for activity detection. Yang *et al.* [13] reported an activity

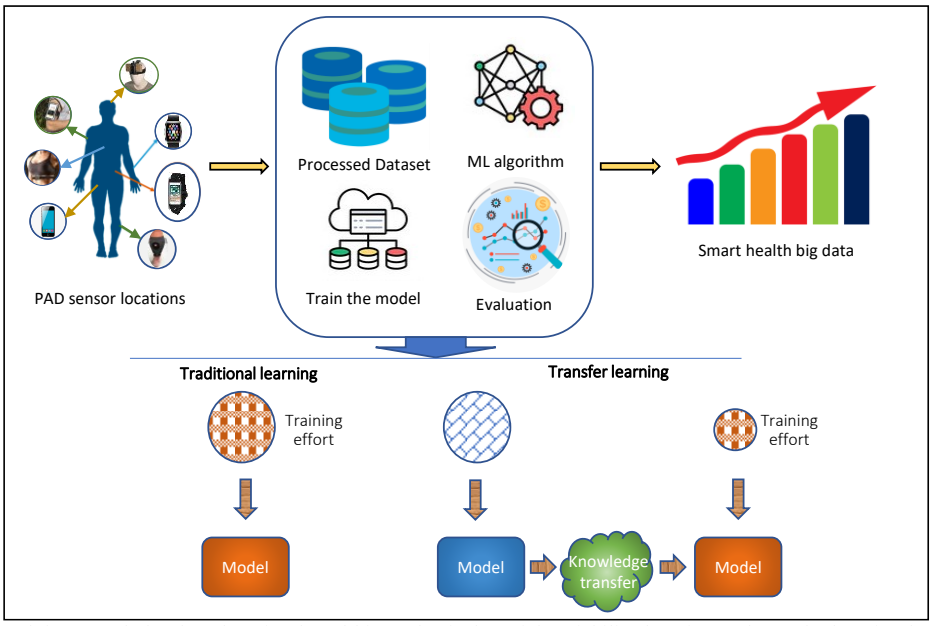

Fig. 1. The proposed novel framework for deep learning-based biomechanical spatial variability learning and transfer learning-based efficient scarce data learning.

graph based on Convolutional Neural Network (CNN). Liu *et al.* reported a support vector machine-based physical activity detection algorithm [14]. Uddin *et al.* reported a random forest-based model for activity and posture recognition [15].

These studies also mainly focus on data analytics and measurement for a single sensor location. We in this study, instead, leverage deep learning to investigate 7 different body locations, for spatial variability characterization. Further, we also characterize each channel of the 3-axis accelerometer and 3-axis gyroscope, resulting in 42 spatial configurations. In our previous study [16], we have studied different sensor locations and indicated the significant spatial variability, and in this study we extend it to a thorough research on 42 different spatial configurations. Another limitation of the previous study is we have not studied the data-efficiency and transfer learning, for scarce data learning.

So, another challenge in this study targets is the data-efficiency in deep learning model training. Typically, deep learning requires a large amount of data for robust model training, which poses significant needs on data collection. Maximizing the data-efficiency for minimizing the training effort on the target user is substantially important but challenging.

Transfer learning studies have been reported in areas like computer vision and natural language processing. For instance, Shaha *et al.* reported the transfer learning model for image classification [17]. Kim *et al.* reported the sequential transfer learning algorithm for lane estimation in self-driving applications [18]. He *et al.* developed a transfer learning model for information recommendation [19].

In biomechanical data analytics, nevertheless, the study of transfer learning [20] is still limited in terms of how to maximize the learning outcomes with minimized training effort. To the best of our knowledge, this is the first study to leverage deep transfer learning on biomechanical data mining for spatial variability characterization and data-efficient learning. Therefore, as another major aim, the transfer learning strategy is introduced in our study to leverage inter-subject similarity for deep learning performance boosting. In such a way, the learned knowledge from other subjects can be transferred to the target user of interest, thereby significantly increasing the physical activity detection (PAD) accuracy of the deep learning model even with no or scarce data from the target user.

Overall, targeting two challenges – spatial variability understanding and scarce data learning, we propose a novel deep transfer intelligence framework (Fig. 1), which leverages deep learning to characterize spatial variability of motion sensors for optimal sensor and channel configuration, and further leverages inter-subject transfer learning to maximize data-efficiency on PAD model training. More specifically, to analyze the spatial variability, we propose the deep convolutional neural network to investigate capabilities of both different sensor locations and different sensor channels, on physical activity detection. The characterization determines both optimal sensor configuration and optimal channel configuration. Further, we propose a transfer learning approach to mine the patterns in the non-target users and then transfer the learned patterns to the target user, thereby minimizing the training effort and maximizing the data-efficiency of the target user. In short, our major contributions are summarized as below:

(a) Propose deep learning algorithms for comprehensively characterizing and understanding the inter-sensor spatial variability for optimal sensor location determination, and inter-channel variability for optimal channel determination, called SwPAD (Sensor-wise PAD) and SCwPAD (Sensor&Channel-wise PAD), respectively;

(b) Determine the optimal sensor location from seven sensor location candidates as thigh, and also determine the optimal sensor&channel configuration from 42 options as

thigh-accelerometer-axis-Y, thereby providing optimal configuration principles for biomechanical measurement;

(c) Propose transfer learning algorithms to extract the patterns from the non-target users and then transfer the learned patterns to the target user (SxPAD corresponds to optimal-sensor-based transfer learning, and SCxPAD corresponds to optimal-sensor&channel-based transfer learning, where x indicates the optimum), for both data-efficiency maximization and model accuracy maximization towards scarce data learning on the target user;

(d) Demonstrate that only 10% of data from the target subject can yield a PAD accuracy up to 91.6%, with the thigh-accelerometer-axis-Y configuration, indicating feasibility of both single-channel-based and scarce-data-based PAD on the target user.

To the best of our knowledge, this is the first time to systematically investigate sensor-wise and channel-wise spatial variability in PAD to determine the optimal sensor location and optimal channel selection, and investigate transferrable patterns in PAD from non-target users to the target user, thereby greatly advancing spatial variability characterization and data-efficient learning in biomechanical measurement.

II. Approaches

We detail in this section the system diagram, optimal sensor determination, optimal sensor&channel determination, data-efficient transfer learning, and evaluation strategy.

A. System Diagram

The proposed system, to deal with the diverse biomechanical dynamics as shown in Fig. 2, aims to firstly determine the optimal sensor and sensor channel configurations through deep mining, and then evaluate the feasibility of transferring knowledge from non-target users to the target user in terms of physical activity detection.

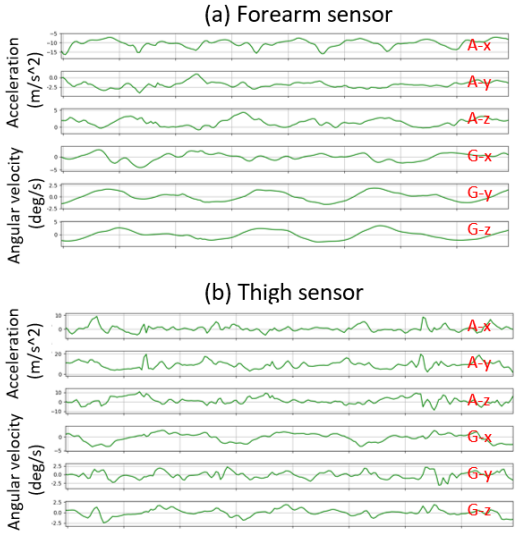

Fig. 2. Selected visualization of six-dimension signal segments during the climbing up activity of the subject 1.
Notes. A: accelerometer; G: gyroscope; X/Y/Z: different signal channels.

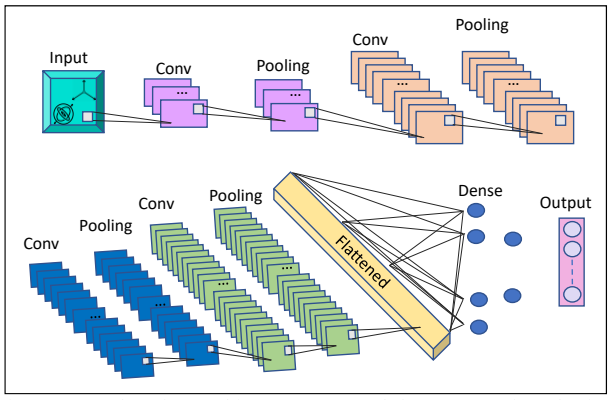

Fig. 3. Deep learning architecture proposed for Sensor-wise Physical Activity Detection (SwPAD), which analyzes the inter-sensor spatial variability to select out the optimal sensor location from seven candidates in this study.

As shown in Fig. 2, the biomechanical data from the forearm sensor and the thigh sensor are highly diverse, and the six channels of each sensor are also of great difference. Therefore, the deep learning architecture as shown in Fig. 3 is proposed to investigate the optimal sensor location, i.e., B. Sensor-wise PAD (SwPAD) for inter-sensor spatial variability analysis. More specifically, seven deep learning models with this same architecture have been trained, corresponding to seven sensor locations in this study. The model architecture includes three convolutional stages, with the number of feature maps as 16, 32, 32, and 64, respectively. The convolutional filter size is set as 1-by-2. After each convolutional stage, there are one max-pooling stage with the pooling operator as 1-by-2, and one dropout stage with the dropping rate as 15%. There are two hidden dense layers and one output layer, with the number of neurons as 512, 256, and 6, respectively. Here the six neurons in the output layer correspond to the number of activity types in this study. For SwPAD, the input dimension is 6-by-100, corresponding to six sensor channels (3-axis accelerometer and 3-axis gyroscope) and the 100-sample signal segment (2 seconds since the sampling rate is 50 Hz). Overall, SwPAD analyzes the inter-sensor spatial variability in terms of physical activity detection performance.

After determining the optimal sensor location from seven candidates in SwPAD, we then name the optimal sensor location as x and then investigate SxPAD – the transfer learning. More specifically, we use data from non-target users to pre-train the deep learning model, with the same architecture in Fig. 3 (input dimension as 6-by-100), and then use different portions of data from the target user to fine-tune the pre-trained model, as shown in Fig. 4. In Fig. 4, the model pre-training uses different portions of data from non-target users, including 0%, 25%, 50%, 75%, and 100%. Then model fine-tuning uses different portions of data from the target user, including 0%, 10%, 20%, 30%, 40%, and 50%. The testing uses 50% of the data from the target users. So there are 29 different strategies (excluding the strategy with 0% for pre-training and 0% for fine-tuning). In this way, we can gain findings on how transfer learning can help minimize the

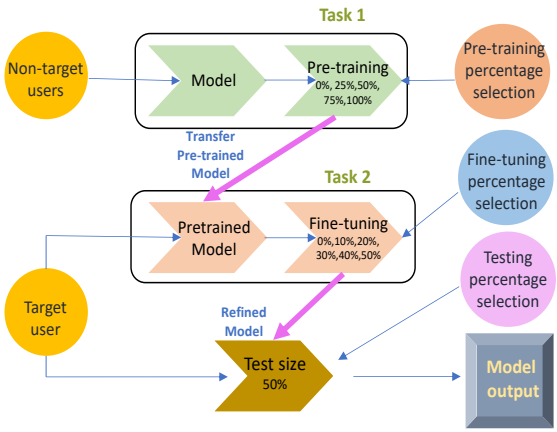

Fig. 4. The proposed transfer learning approach, which pre-trains the model on the non-target users and then fine-tunes the model on the target user, to facilitate PAD performance on the target user towards efficient scarce data learning.

requirement of data from the target user, and how transfer learning can boost the performance.

Further, we have investigated the sensor&channel configurations. 42 combinations are considered, since there are seven sensor locations and six channels for each location (3-axis accelerometer and 3-axis gyroscope), resulting in Sensor&Channel-wise PAD (SCwPAD). The deep learning architecture is also like Fig. 3, but the input dimension is 1-by-100 since there is only one channel selected for each configuration. In total, 42 models have been trained and the optimal sensor&channel configuration is determined.

Based on the optimal sensor&channel configuration, x, we have further studied the transfer learning, still shown as Fig. 4, i.e., SCxPAD, with the same deep learning architecture and the input dimension is set as 1-by-100. SCxPAD is expected to minimize the training effort and maximize the data-efficiency through both single-channel-based learning and transfer learning.

B. Sensor-wise Physical Activity Detection (SwPAD) for Inter-sensor Spatial Variability Analysis

To investigate the inter-sensor spatial variability, we have proposed a CNN architecture as shown in Fig. 3, which includes the convolutional filters for spatial pattern extraction, max-pooling operators for dimension reduction, and fully connected dense layers for final class label generation from flattened patterns.

The learning principle of CNN [21-24] is as (1), and $z_{i,j}^{l,k}$ is corresponding to the $i-th$ row and $j-th$ column of the $k-th$ feature map in the layer l, which is calculated as the sum of the weighted neuron output $y_{i+m,j+n}^{l-1,c}$ in the previous layer with the weight as $w_{m,n,c}^{l,k}$. M, N, and C are filter height, filter width, and number of input maps, respectively, and m, n, and c are their corresponding indices. b is the bias input for the neuron. After feeding $z_{i,j}^{l,k}$ into the activation function $\varphi(\cdot)$, which is chosen as 'RELU' for computation efficiency, the neuron output $y_{i,j}^{l,k}$ is yielded as (2).

$$z_{i,j}^{l,k} = \sum_{m=0}^{M-1}\sum_{n=0}^{N-1}\sum_{c=0}^{C-1} w_{m,n,c}^{l,k} y_{i+m,j+n}^{l-1,c} + b \quad (1)$$

$$y_{i,j}^{l,k} = \varphi\left(z_{i,j}^{l,k}\right) \quad (2)$$

With the backpropagation learning algorithm and the chain rule of differentiation, the gradient of the error E with respect to the convolutional filter weight $w_{m,n,c}^{l,k}$ is given as (3), where the E is backpropagated to $z_{i,j}^{l,k}$ and then to $w_{m,n,c}^{l,k}$. H and W are the height and width of the $k-th$ feature map in the layer l. After further derivation, (3) is transformed to be (4), where $\delta_{i,j}^{l,k}$ is the gradient of E with respect to the input of the activation function.

$$\frac{\partial E}{\partial w_{m,n,c}^{l,k}} = \sum_{i=0}^{H-M}\sum_{j=0}^{W-N} \frac{\partial E}{\partial z_{i,j}^{l,k}} \frac{\partial z_{i,j}^{l,k}}{\partial w_{m,n,c}^{l,k}} \quad (3)$$

$$\frac{\partial E}{\partial w_{m,n,c}^{l,k}} = \sum_{i=0}^{H-M}\sum_{j=0}^{W-N} \delta_{i,j}^{l,k} y_{i+m,j+n}^{l-1,c} \quad (4)$$

We will leverage the proposed CNN deep learning model to evaluate seven different sensor locations and determine the performance in terms of physical activity detection. The total number of parameters is 1.3 million. The model has four CNN stages (16, 32, 32, and 64 feature maps, respectively) and three dense layers (512, 256 and 6, respectively), as shown in Fig. 3. The spatial variability is reflected by the PAD performance with seven different models (corresponding to seven different sensor locations).

C. Optimal Sensor Location x Determination after SwPAD

The optimal sensor determination is achieved by (5), where the 6-axis data from sensor x, denoted as S_x, is fed into the CNN model $f(\cdot)$. The performance is then calculated with the function $Accuracy(\cdot)$ which is calculated as the number of correctly classified instances divided by the total number of instances, and the optimax sensor index x^* is finally determined.

$$x^* = \underset{x}{argmax}[Accuracy(f(S_x))] \quad (5)$$

Considering the spatial variability among seven sensor locations, chest, forearm, head, shin, thigh, upper-arm, and waist, the proposed deep learning model is expected to be able to effectively mine these diverse biomechanical dynamics and determine their contribution to the physical activity detection task. Looking forward, for more diverse biomechanical dynamics-based applications like rehabilitation, assisted prosthesis, and movement disorders, the proposed deep learning model is expected to be able to find out the most effective sensor location that can maximize both information capturing and detection accuracy.

D. Transfer Learning (SxPAD) from Non-target Users to The Target User, with the Selected Optimal Sensor Location x

Further, we propose a transfer learning [25-29] approach to maximize the deep learning performance and minimize the

training effort, based on the optimal sensor location, named as SxPAD. The achieved methodology, as shown in Fig. 4, therefore, can boost the deep learning accuracy through shared inter-subject dynamics. More specifically, when selecting a subject as the target user, we define other subjects as the non-target users. For the whole dataset, we repeat this for each subject, meaning that each subject can be the target user. The transfer learning SxPAD is still based on the same CNN (input is 6-by-100), but trained in a different strategy with two steps as below.

In the first step, the model is pre-trained with the data from non-target users; and in the second step, the model is fine-tuned with the data from the target user. Different proportions of the pre-training data and different proportions of the fine-tunning data have been considered, resulting in 29 transfer learning strategies (removing the case with 0% for pre-training and 0% for fine-tuning). So, 29 models have been evaluated independently. Fig. 4 gives the overall approach in deep transfer learning, and the detailed algorithm is given in Algorithm 1, where TL-OPTE, which stands for "Transfer Learning for Optimal Performance and Training Effort", is proposed.

The TL-OPTE algorithm, starting with the minimum amount (ψ_i) of data from the target user (Ω^t), evaluates and determines an appropriate amount (ϕ_i) of data from non-target users (Ω^{nt}), which can achieve performance equal to or above a pre-defined threshold (ε_{th}).

As shown in the algorithm, given the initial deep learning model π, and several sets of parameters, the algorithm will finally output the indicator (γ) of whether the optimal solution is found, the trained model (π^*), and generated optimal configurations like percentage of data needed for pre-training ϕ^* and percentage of data needed for fine-tuning ψ^*. Different pre-defined thresholds (ε_{th}) have been evaluated in the results.

The proposed algorithm firstly focuses on $\psi_i = 0$, i.e., no need of target data, and evaluates different amounts of non-target data (for ϕ_i in Φ) to determine the optimal percentage. The model in these cases is only pre-trained with non-target data without fine-tuning. If the performance meets the requirement ε_{th}, the algorithm returns the solution and stops. Otherwise, the algorithm increases the amount of target data, and fine-tunes the pre-trained model with this available target data for possible performance enhancement.

This process iterates until the optimal solution is determined, or the algorithm outputs the indicator showing that no solutions found and suggests that, either a different performance threshold should be chosen to relax the requirement, or a different deep learning architecture should be considered to enhance the performance.

One thing to note is that the optimal percentage for the non-target data may be the smaller one, not the highest one, which will be further analyzed in the results section. This is because the diversity of the inter-subject similarity may have negative impacts on the model pre-training. So, there is an optimal tradeoff between leveraging the inter-subject similarity and avoiding an over-pre-trained model.

We in future will also study how to incorporate deep learning model architecture enhancement in the proposed algorithm. In this study, one of the efforts is to demonstrate the effectiveness of the TL-OPTE algorithm in terms of performance maximization and training effort minimization with a pre-designed deep learning model.

Algorithm 1 TL-OPTE
(Transfer Learning for Optimal Performance and Training Effort)

Input:
initial deep learning model π
non-target dataset Ω^{nt}
set of percentage for non-target dataset $\Phi = \{\phi_i | i = 0, \dots, 100\%\}$
target dataset Ω^t
set of percentage for target dataset $\Psi = \{\psi_i | i = 0, \dots, 50\%\}$
percentage of target data for testing τ
performance threshold ε_{th}

Output:
indicator of whether optimal solution found γ
optimal deep learning model π^*
percentage of data needed for pre-training ϕ^*
percentage of data needed for fine-tuning ψ^*
performance of the optimal deep learning model μ^*

Procedure:
$\gamma = FALSE; \pi^* = \pi; \phi^* = 0; \psi^* = 0; \mu^* = 0$ //initialization
for ψ_j **in** Ψ **do** //loop ψ_j in target user' data Ψ
  for ϕ_i **in** Φ **do** //loop ϕ_i in non-target users' data Φ
    if ($\psi_j == 0\%$) **and** ($\phi_i == 0\%$) **do**
      pass //pass the case that has no data
    else do
      if ($\phi_i > 0\%$) **do**
        $\pi = \Gamma(\pi, \Omega^{nt}, \phi_i)$ //pre-train the model π
      end if
      if ($\psi_i > 0\%$) **do**
        $\pi = \Gamma(\pi, \Omega^{t}, \psi_j)$ //fine-tune the model π
      end if
      $\mu_{i,j} = \rho(\pi, \Psi, \tau)$ //performance calculation
      if $\mu_{i,j} >= \mu^*$ **do**
        $\phi^* = \phi_i; \mu^* = \psi_j$ //optimal percentage determined
        $\pi^* = \pi; \mu^* = \mu_{i,j}$ //optimal model determined
        $\gamma = True$
      end if
    end if
  end for
  if ($\gamma == True$) **and** ($\mu^* \geq \varepsilon_{th}$) **do** //optimal configurations found
    break
  end if
end for
return $\gamma, \pi^*, \phi^*, \psi^*, \mu^*$ //optimal model, configuration, performance

E. Sensor&Channel-wide Physical Activity Detection (SCwPAD) for Inter-sensor&channel Spatial Variability Analysis

To further investigate the spatial variability in multi-channel

signals of each sensor location, we propose to leverage deep learning to quantify the contribution of each sensor&channel combination in the physical activity detection task. Considering seven sensor locations and six signal channels per sensor (3-axis acceleration and 3-axis angular velocity), we have studied 42 deep learning models to analyze the spatial variability, and determine the optimal sensor&channel configuration.

The deep learning model is also based Fig. 3 for fair comparison purpose, with the difference in the number of input channels which is six for SwPAD and one for SCwPAD.

F. Optimal Sensor&Channel Configuration x Determination after SCwPAD

The optimal sensor&channel configuration is determined by (6), where each configuration SC_x is fed into the CNN model $f(\cdot)$, and the performance is calculated as $Accuracy(\cdot)$ which is calculated as the number of correctly classified instances divided by the total number of instances. The determined configuration x^* then indicates the sensor location and the signal channel that can represent the major patterns under different physical actiivty types.

$$x^* = \underset{x}{\text{argmax}}[Accuracy(f(SC_x))] \quad (6)$$

This not only selects out the best configuration for biomechanical dynamics representation, but also provides an efficient way for minimizing the training effort and energy requirements, towards pervasive wearable smart health.

G. Transfer Learning (SCxPAD) from Non-target Users to The Target User, with the Selected Optimal Sensor&Channel Configuration x

We have further investigated the transfer learning approach based on the optimal sensor&channel configuration, names as SCxPAD. The same algorithm TL-OPTE is applied to determine the optimal learning strategy for performance maximization and training effort minimization. For transfer learning SCxPAD, the same deep learning model as Fig. 3 is used with the input dimension as 1-by-100. Also, different portions of the pre-training data and fine-tuning data have been considered, resulting in also 29 transfer learning strategies.

The difference of applying TL-OPTE on SCxPAD and SxPAD is that, the former one uses 1-channel datasets, for both non-target users and the target user. The major algorithm flow is the same. The algorithm finally outputs the optimal model, configuration and performance after automatically and quantitatively searching the solution space.

H. Evaluation Strategy

To thoroughly evaluate the proposed algorithm framework, we will firstly demonstrate the results of SwPAD for optimal sensor location determination. Further, we will demonstrate the optimal of sensor&channel configuration under SCwPAD. Finally, we will show the transfer learning under SxPAD and SCxPAD, respectively.

III. RESULTS

A. Experimental Setup

The proposed framework has been evaluated on comprehensive sensor locations and signal channels, with different daily activity types. The multi-location multi-type motion database [30] is used, which has included seven sensor locations (chest, forearm, head, shin, thigh, upper arm, and waist), two 3-axis sensors (accelerometer and gyroscope) per location, and six activity types (climbing downstairs, climbing upstairs, jumping, lying, running/jogging, and walking). Each of fifteen subjects performed each activity for approximately 10 minutes (except for jumping, about 2 minutes). The signal was sampled at 50Hz and is segmented every 100 samples, which is same as the input width of the CNN model.

The simulation has been conducted o n the Dell Laptop with Nvidia GPU-based deep learning training and testing. The number of epochs is selected as 80. The training/testing splitting in spatial variability learning is set as 80%/20%. In deep transfer learning, the splitting is based on the approach given in Fig. 4, and explored by the proposed Algorithm 1: TL-OPTE. The six activity types have similar length of recording, except running. Considering running has sig nificant fluctuations of the signal amplitude which will facilitate learning already, no special data enhancement has been made to this minority class. Fro m the reported performance next, we can also observe all activity types have been effectively detected.

B. SwPAD for Inter-sensor Spatial Variability Analysis

The SwPAD learning outcomes are demonstrated in Fig. 5 and Fig. 6. We have split the instances of each subject to 80% and 20%, for training and testing, respectively. User-specific models have been trained and tested. As shown in Fig. 5, the learning process of selected sensor locations has converged well with continuously reduced training loss, indicating the effectiveness of the CNN deep model. With 80 epochs, the learning loss has effectively decreased and become stable, and the high testing accuracy is further given in Fig. 6.

In Fig. 6, selected confusion matrices and performance summary for the thigh and upper arm locations, under SwPAD, are demonstrated. The comparison indicates much better performance with the thigh sensor location. The average accuracy of this thigh location is up to 98%. The recall,

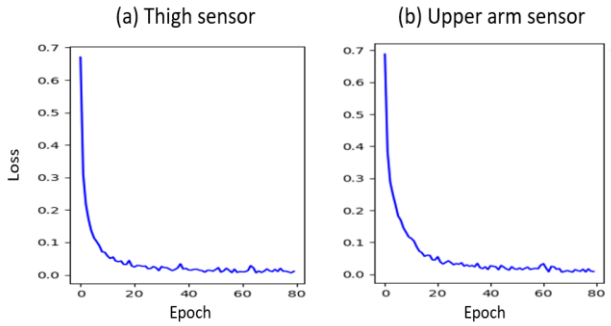

Fig. 5. The convergence of deep learning for (a) thigh sensor, and (b) upper arm sensor, under SwPAD.

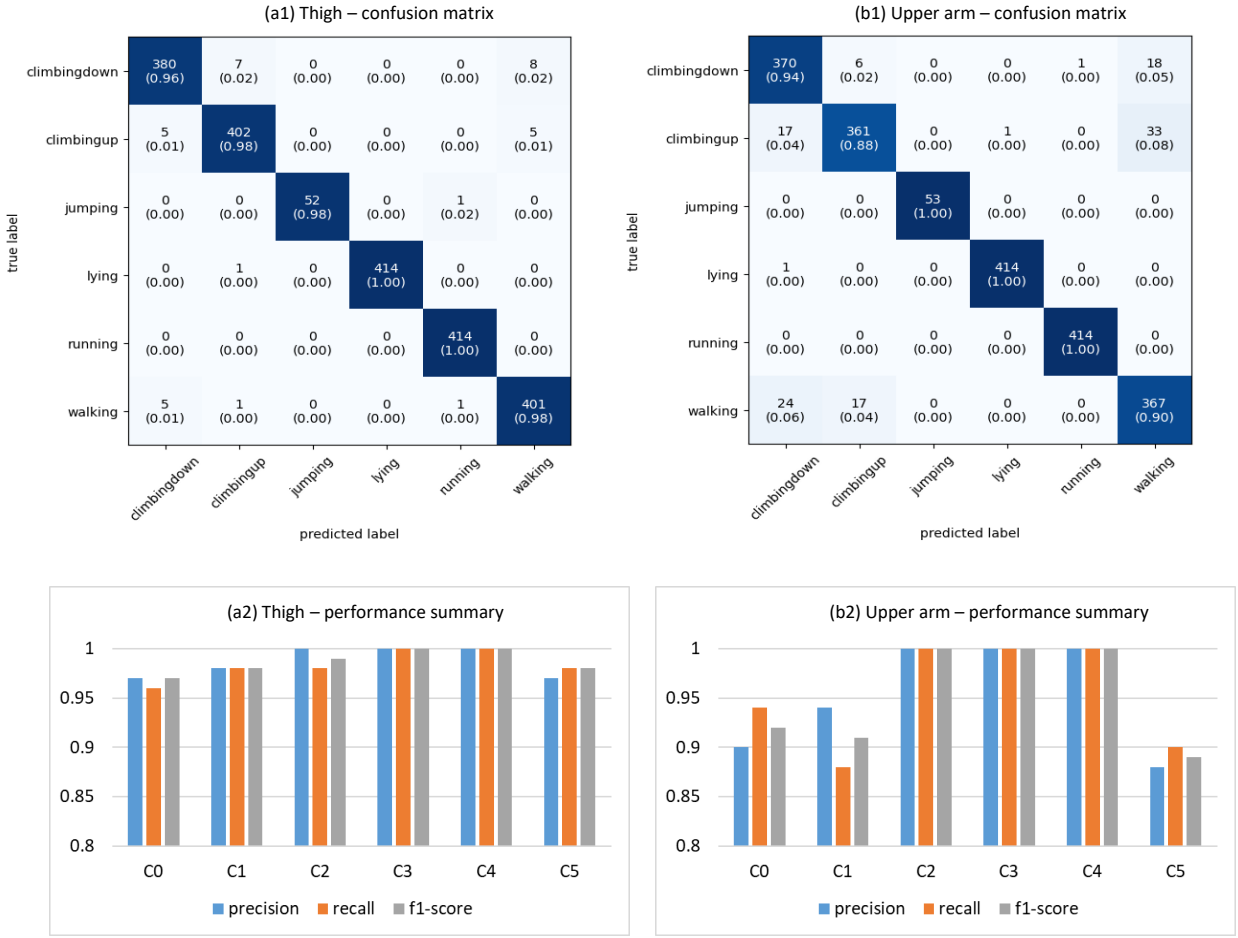

Fig. 6. Selected confusion matrices and performance summary for the thigh and upper arm locations, under SwPAD. The comparison indicates much better performance for the thigh sensor location, which will be further analyzed in Fig. 7 which summarizes the performance for all seven sensor locations.
Note. C0 to C5: six different classes, corresponding to climbing downstairs, climbing upstairs, jumping, lying, running/jogging, and walking, respectively.

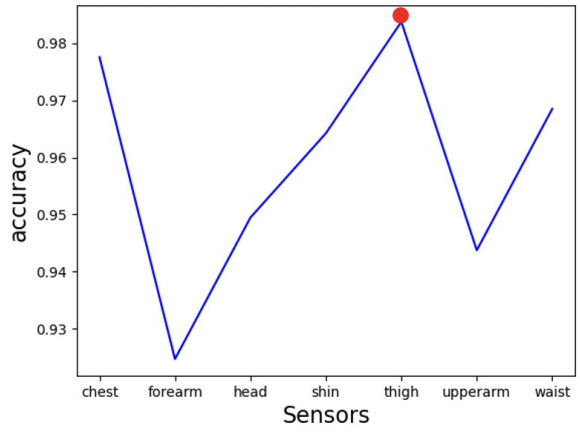

Fig. 7. Accuracy ranking plot of all seven sensor locations under SwPAD. The highest accuracy is obtained at the thigh sensor location, among all seven sensor locations.

precision, and f1-score are all above 95% for six different activity types, resulting in an average performance improvement of 4% compared with the upper arm location. The SwPAD analysis has given the PDA performance for each of the seven sensor locations, which will be further analyzed in the next step to determine the optimal sensor location *x*.

C. SwPAD Summary and Optimal Sensor Location x Determination

To summarize the performance of SwPAD, in Fig. 7, the performance of seven sensor locations, averaged on fifteen subjects, is given. The accuracy is used here, considering other criteria have similar trend as the accuracy, as shown in Fig. 6. From the demonstration, we can observe that all seven locations have an accuracy above 90%. The chest and thigh locations are top two among seven options. This could result from the relatively consistent biomechanical dynamics compared with other locations like forearm and upper arm. The tradeoff may therefore need to be made between the wearability and the convenience. Besides, the thigh location may be a more convenient location compared with the chest location. The accuracy of thigh is around 98.5%, averaged on fifteen subjects, so thigh is selected as the optimal sensor location. We will then, further investigate the difference among six signal channels of each sensor location.

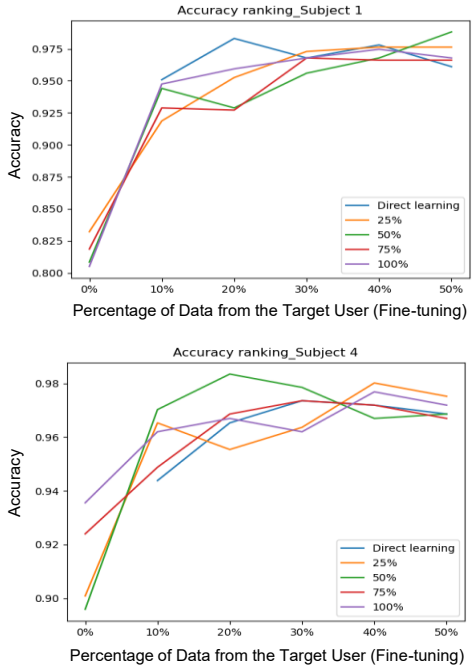

Fig. 8 Selected accuracy ranking plots (subject 1 and 4) from transfer learning SxPAD, i.e., the transfer learning on the optimal sensor location (thigh).
Notes. (1) The percentage (0%, 25%, 50%, 75%, 100%) in the legend: amount of data from non-target users for pre-training the transferable model, where 0% is 'Direct learning' without transfer learning.
(2) The percentage (0%, 10%, 20%, 30%, 40%, 50%) on the horizontal axis: amount of data from the target user for model fine-tuning. The accuracy is reported based on 50% of the data from the target user for each case.

D. Transfer Learning (SxPAD) from Non-target Users to The Target User, with the Selected Optimal Sensor Location x

We will then investigate the transfer learning approach for both SxPAD, and SCxPAD. Here we firstly focus on SxPAD. In Fig. 8, two examples of the transfer learning outcomes are given. The percentage (0%, 25%, 50%, 75%, 100%) in the legend indicates the amount of data from non-target users for pre-training the transferable model, where 0% is labeled as 'Direct learning', i.e., without transfer learning. The percentage (0%, 10%, 20%, 30%, 40%, 50%) on the horizontal axis provides the amount of data from the target user for model fine-tuning. The accuracy is reported based on 50% of the data from the target user for each case. The data from the thigh sensor location is used here. In direct learning, only the target user data is used in training.

There are several major findings. Firstly, when without fine-tuning (horizontal axis = 0%), the accuracy of pre-trained models, tested on the target user, can already achieve an accuracy between 80% and 94%. It indicates the inter-subject similarity has been well learned. Secondly, the amount of data used in pre-training has not shown strong consistency when related to the performance. For example, in the top graph, 25% pre-training is best for user 1, while in the bottom graph, 100% pre-training is best for user 4. This may result from the diverse inter-subject similarity, which, if high enough, will contribute to the performance like the bottom graph. Thirdly, when introducing 10% of target data for fine-tuning, the performance boosts significantly. With more target data for fine tuning, the performance keeps increasing.

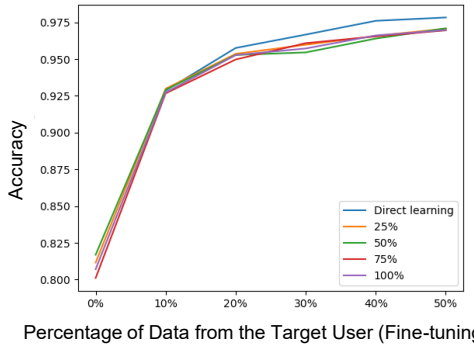

Fig. 9. Average accuracy ranking plots for transfer learning SxPAD, with the determined optimal location (thigh).
Note. Same definition of the legend (pre-training percentage) and horizontal axis (fine-tuning percentage) as Fig. 8.

To better summarize the transfer learning performance over all fifteen subjects, Fig. 9 gives the average accuracy, meaning that each subject has been treated as the target user and the other subjects as non-target users. Considering randomness of deep learning training, each transfer learning strategy has been evaluated twice and then averaged here. Still, we can observe that the accuracy is around 80% to 82.5% when without fine-tuning. With 10% fine-tuning, the performance is boosted to around 92.5%.

One thing to mention is that, the direct learning (without transfer learning) has an accuracy a bit higher than pre-training&fine-tuning, which should result from the inter-subject difference that may lower the performance slightly when more target data is used. However, we expect to observe different results for SCxPAD, considering that the single-channel data of the target user may not be enough for model training and the transfer learning will significantly benefit the single-channel cases. It is detailed in the section F.

E. SCwPAD Summary and Optimal Sensor&Channel Configuration x Determination

As shown in Fig. 10, 42 combinations of seven sensor locations and six channels per location have been evaluated and visualized, which give the difference of each configuration in terms of physical activity detection.

To the best of our knowledge, it is the first study to comprehensively compare these configurations and reveal their ability in biomechanical dynamics mining. As shown, the chest and thigh locations, even with single signal channel, are still among the top configurations. Besides, the accelerometer-channel Y is the best case for these two locations.

Considering the thigh location is the optimal choice among 6-channel sensor configurations under SwPAD, and the performance for thigh based on accelerometer-channel Y is comparable to that of chest, we finally select the 'thigh& accelerometer-channel Y' as the optimal configuration.

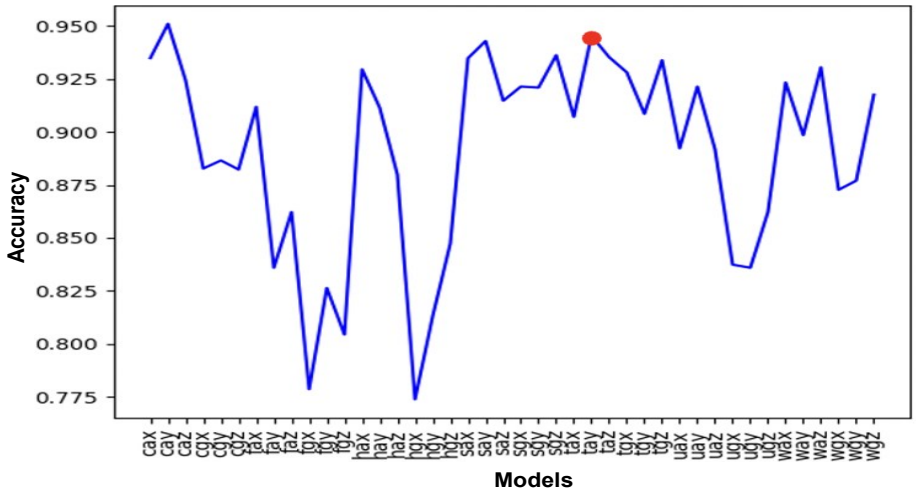

Fig. 10. Accuracy ranking plot of all 42 sensor & channel combinations (7 sensors * 6 channels/location) under SCwPAD.
Notes. (1) Each deep learning model on the horizontal axis is represented by three letters, e.g., 'tay' explained above. The first letter has six possibilities: c/f/h/s/t/u/w, which stand for chest/forearm/head/shin/thigh/upper-arm/waist, respectively.
(2) The second letter has two possibilities: a/g, which stand for the accelerometer/gyroscope sensor, respectively.
(3) The third letter has three possibilities: X/Y/Z, which stand for three different channels of a given sensor.

F. Transfer Learning (SCxPAD) from Non-target Users to The Target User, with the Selected Optimal Sensor&Channel Configuration x

Transfer learning is attractive in sharing the knowledge from non-target users to the target user when the target data is limited. We here have studied the transfer learning under SCxPAD. Selected examples about two subjects are shown in Fig. 11, indicating the effectiveness of transfer learning for single-channel-based physical activity detection task. The average accuracy ranking plots for all subjects are given in Fig. 12. Detailed analysis of these figures is given below.

In Fig. 11, there are several interesting findings. Firstly, the accuracy without fine-tuning (horizontal axis=0%) is already between 86% and 92%, indicating that the inter-subject similarity for the single-channel scenarios (SCxPAD) is more consistent than that for the 6-channel scenarios (SxPAD). This indicates that the accelerometer-channel Y is of critical biomechanical dynamics, and further introducing other channels, may lower the perfor mance due to the complexity of the inter-subject similarity.

Secondly, the accuracy without fine-tuning (horizontal axis=0%) is much higher than the accuracy under 10% of direct learning. This further indicates the inter-subject similarity is pretty high for the thigh&accelerometer-channel

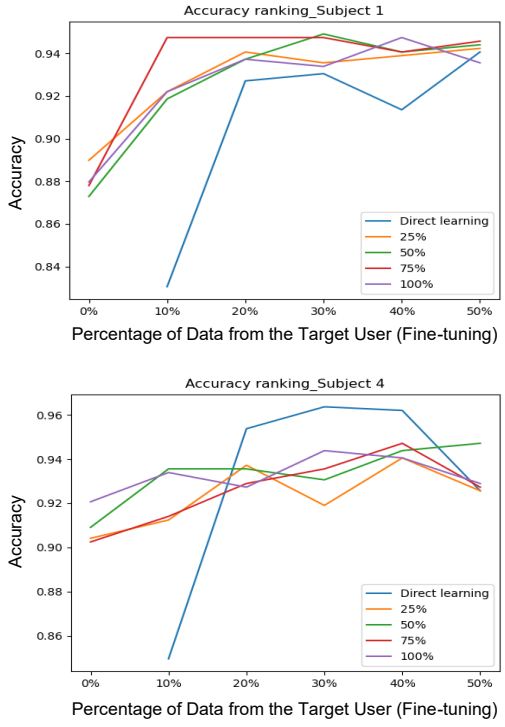

Fig. 11. Selected accuracy ranking plots (subject 1 and 4) for transfer learning SCxPAD, with the determined optimal sensor&channel configuration (thigh-accelerometer-channel Y).
Note. Same definition of the legend (pre-training percentage) and horizontal axis (fine-tuning percentage) as Fig. 8.

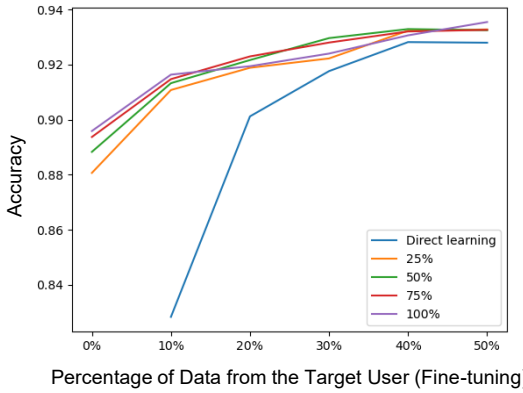

Fig. 12. Average accuracy ranking plots for transfer learning SCxPAD, with the determined optimal sensor&channel configuration (thigh-accelerometer-channel Y).
Note. Same definition of the legend (pre-training percentage) and horizontal axis (fine-tuning percentage) as Fig. 8.

Y configuration.

Thirdly, when increasing the percentage of fine-tuning effort, different subjects may or may not benefit much from pre-training. This further indicates the complexity of inter-subject similarity.

Overall, encouragingly, the average performance on all subjects shown in Fig. 12, demonstrates transfer learning significantly improves the performance of direct learning on the target user. Considering randomness of deep learning training, each transfer learning strategy has also been evaluated twice and then averaged here. By setting different performance thresholds as shown in Table I, the corresponding optimal solutions are determined by the proposed TL-OPTE algorithm under SCxPAD.

The results in Table I indicates that the optimal pre-training effort ϕ^* may not always be 100% for trading off between learning inter-subject similarity and avoiding over-pre-training, and the fine-tuning effort ψ^* can be very small for training effort minimization. Further the optimal accuracy μ^* can be higher than the threshold.

Our experiments have further demonstrated that, with transfer learning, only 10% of data from the target subject can yield a physical activity detection accuracy up to 91.6%. This indicates the deep transfer learning framework has enabled very challenging scarce data learning on the target user, not only for minimizing the training effort on the target, but also for increasing the model performance on the target with transferred knowledge.

In short, the proposed transfer learning framework can effectively maximize the performance and minimize the training effort on the target user, by optimally leveraging the inter-subject similarity to learn the sharable knowledge and patterns.

G. Comparison with Previous Studies

To further illustrate the spatial variability learning and scarce data learning with the proposed framework, we have conducted detailed comparison with other studies. Panahandeh *et al.* [4] placed the motion sensor on the chest; Kim *et al.* [31] placed the sensor on the wrist; Kang *et al.* [32] put the sensor on the arm; Zou *et al.* [5] put the sensor on the elbow. However, there is no comprehensive study on biomechanical spatial variability learning.

In our study, with the same experiment setting up, we have fairly and thoroughly compared different sensor locations and channels, and determined the optimal system configuration principle.

Further, previously studies also reported motion signal processing algorithms, such as Hidden Marko Model [4], Kalman Filtering [11], Long Short-term Memory [7] and CNN [13]. However, no study has been reported on deep transfer learning of the biomechanical data, towards the scarce data learning challenge. In this study, we have proposed and validated a deep transfer learning framework, and conducted thorough evaluations to demonstrate the effectiveness.

With our algorithm, even with 10% of the target data, we can achieve satisfied performance through transferring the knowledge from non-target users. We have also demonstrated the scarce data learning in direct learning (without transferring knowledge from non-target users), as shown in Fig. 11 and Fig. 12. The simulation shows that, only 10% of the target user data is not enough for learning an effective model since the performance drop is about 9%. Therefore, this study will greatly advance scarce data learning in wearable health instrumentations, considering the data collection is time-consuming and the inconvenient.

Table I. The optimal solutions determined by the proposed TL-OPTE algorithm, under SCxPAD. Take the performance threshold $\varepsilon_{th} =$ 90% as an example, with transfer learning, only 10% of data from the target subject can yield a physical activity detection accuracy up to 91.6%, with a performance boosting of 9% compared with direct learning without transfer learning.

ε_{th}	ϕ^*	ψ^*	μ^*
86%	100%	0%	89.6%
88%	100%	0%	89.6%
90%	**100%**	**10%**	**91.6%**
92%	75%	20%	92.3%
93%	50%	30%	93.0%

Notes.
(1) ε_{th}: performance threshold; ϕ^*: percentage of data needed for pre-training; ψ^*: percentage of data needed for fine-tuning; μ^*: performance of the optimal deep learning model.
(2) The granularity for the percentages (ϕ^* and ψ^*) will provide can be further fine-grained based on the requirement, which can facilitate further minimization of the pre-training and fine-turning effort.

H. Limitations and Future Studies

We will further implement the proposed algorithm on the edge computing platform, e.g., the smartphone or wearable monitor. In the current study, the training and testing have both been done on a PC workstation with NVIDIA RTX A4000 GPU. One thing to note is that the deep transfer learning framework only increases the computation load in the training process, and does not increase the computation load of the deep neural network when implemented on the edge platform. Besides, the convolutional neural network can be efficiently supported by the processors on the edge platform, thanks to its regular paralleling processing flow and the shared convolutional weights for the same kernel.

Besides, the contributions of each block in the network are also interesting, not only to evaluate the robustness of the network, but also to further design an efficient light-weight model. In this study, we have mainly targeted the spatial variability understanding and the scarce data learning, which can be further enhanced in the ablation experiments and studies in future.

In future, we will also continue studying effective deep learning algorithms and transfer learning approaches to further enhance the accuracy and minimize the learning effort. Further, incorporating deep learning architecture search in the proposed TL-OPTE algorithm will also be interesting, which can facilitate automatic architecture determination for both performance improvement and model size reduction. Human

subjects are of great diversity in not only biomechanical big data but also other modalities [33-36], and it will be promising to advance the proposed framework to more smart health applications [37-40]. The proposed framework is of a high generalization capability, considering the spatial variability learning among sensors is a common need, and also the transfer learning is important for the scarce data learning challenge in wearable applications. We in the future will further enhance the framework on diverse sensing modalities and scenarios.

We will also further study more sensor locations in future, which will facilitate enhanced understanding of the spatial variability and optimal sensor selection. Also, deep transfer learning may have different effects on different sensor locations.

IV. Conclusion

In this research, targeting biomechanical dynamics measurement that is of great promise for rehabilitation, assisted-living, and lifestyle management applications, we have proposed a deep transfer learning framework that can effectively grasp the inter-sensor spatial variability and inter-subject similarity. The novel framework, for the first time, not only reveals the optimal sensor location from seven candidates and optimal sensor&channel combination from 42 candidates, but also demonstrates how transfer learning maximizes the data-efficiency in physical activity detector learning. Our evaluation experiments have determined the optimal sensor location as thigh, and the optimal sensor&channel configuration as thigh-accelerometer-axis-Y. Our experiments have further demonstrated that, with transfer learning under the optimal sensor&channel configuration, only 10% of data from the target subject can yield a physical activity detection accuracy up to 91.6%. This indicates the deep transfer learning framework has enabled very challenging scarce data learning on the target user, not only for minimizing the training effort on the target, but also for increasing the model performance on the target with transferred knowledge. Targeting the limitations of this study, we in future will further study the implementation of the algorithm on mobile devices, investigate the ablation effects, evaluate the algorithm on more data modalities and scenarios, and study more sensor locations. The research will greatly advance spatial variability characterization and data-efficient learning in biomechanical measurement.

References

[1] CDC. "Disability Impacts All of Us." https://www.cdc.gov/ncbddd/disabilityandhealth/infographic-disability-impacts-all.html (accessed.

[2] U. Census. "Disability Rates Highest Among American Indian and Alaska Native Children and Children Living in Poverty." https://www.census.gov/library/stories/2021/03/united-states-childhood-disability-rate-up-in-2019-from-2008.html (accessed.

[3] S. Shirmohammadi, K. Barbe, D. Grimaldi, S. Rapuano, and S. Grassini, "Instrumentation and measurement in medical, biomedical, and healthcare systems," *IEEE Instrumentation & Measurement Magazine,* vol. 19, no. 5, pp. 6-12, 2016.

[4] G. Panahandeh, N. Mohammadiha, A. Leijon, and P. Händel, "Continuous hidden Markov model for pedestrian activity classification and gait analysis," *IEEE Transactions on Instrumentation and Measurement,* vol. 62, no. 5, pp. 1073-1083, 2013.

[5] G. X. Lee, K. S. Low, and T. Taher, "Unrestrained measurement of arm motion based on a wearable wireless sensor network," *IEEE transactions on instrumentation and measurement,* vol. 59, no. 5, pp. 1309-1317, 2010.

[6] H. Zhou and H. Hu, "Reducing drifts in the inertial measurements of wrist and elbow positions," *IEEE Transactions on Instrumentation and Measurement,* vol. 59, no. 3, pp. 575-585, 2009.

[7] S. Ashry, T. Ogawa, and W. Gomaa, "CHARM-deep: Continuous human activity recognition model based on deep neural network using IMU sensors of smartwatch," *IEEE Sensors Journal,* vol. 20, no. 15, pp. 8757-8770, 2020.

[8] M. Abid, N. Mezghani, and A. Mitiche, "Knee joint biomechanical gait data classification for knee pathology assessment: a literature review," *Applied Bionics and Biomechanics,* vol. 2019, 2019.

[9] M. M. McCulloch *et al.*, "Biomechanical modeling of radiation dose-induced volumetric changes of the parotid glands for deformable image registration," *Physics in Medicine & Biology,* vol. 65, no. 16, p. 165017, 2020.

[10] A. Nasr *et al.*, "MuscleNET: mapping electromyography to kinematic and dynamic biomechanical variables by machine learning," *Journal of Neural Engineering,* vol. 18, no. 4, p. 0460d3, 2021.

[11] J. Li *et al.*, "Using body sensor network to measure the effect of rehabilitation therapy on improvement of lower limb motor function in children with spastic diplegia," *IEEE Transactions on Instrumentation and Measurement,* vol. 69, no. 11, pp. 9215-9227, 2020.

[12] H. Ahmed and M. Tahir, "Improving the accuracy of human body orientation estimation with wearable IMU sensors," *IEEE Transactions on instrumentation and measurement,* vol. 66, no. 3, pp. 535-542, 2017.

[13] P. Yang, C. Yang, V. Lanfranchi, and F. Ciravegna, "Activity Graph based Convolutional Neural Network for Physical Activity Recognition using Acceleration and Gyroscope Data," *IEEE Transactions on Industrial Informatics,* 2022.

[14] S. Liu, R. X. Gao, D. John, J. Staudenmayer, and P. S. Freedson, "SVM-based multi-sensor fusion for free-living physical activity assessment," in *2011 Annual International Conference of the IEEE Engineering in Medicine and Biology Society*, 2011: IEEE, pp. 3188-3191.

[15] M. T. Uddin, M. M. Billah, and M. F. Hossain, "Random forests based recognition of human activities and postural transitions on smartphone," in *2016 5th International Conference on Informatics, Electronics and Vision (ICIEV)*, 2016: IEEE, pp. 250-255.

[16] K. Gangadharan and Q. Zhang, "Deep Learning of Biomechanical Dynamics With Spatial Variability for Lifestyle Management," in *2022 IEEE 4th Global Conference on Life Sciences and Technologies (LifeTech)*, 2022: IEEE, pp. 514-515.

[17] M. Shaha and M. Pawar, "Transfer learning for image classification," in *2018 second international conference on electronics, communication and aerospace technology (ICECA)*, 2018: IEEE, pp. 656-660.

[18] J. Kim and C. Park, "End-to-end ego lane estimation based on sequential transfer learning for self-driving cars," in *Proceedings of the IEEE conference on computer vision and pattern recognition workshops*, 2017, pp. 30-38.

[19] M. He, J. Zhang, and J. Zhang, "MINDTL: Multiple incomplete domains transfer learning for information recommendation," *China Communications,* vol. 14, no. 11, pp. 218-236, 2017.

[20] J. Zou and Q. Zhang, "eyeSay: Make Eyes Speak for ALS Patients with Deep Transfer Learning-empowered Wearable," in *IEEE EMBS Annual Conference* 2021: IEEE.

[21] Y. LeCun, Y. Bengio, and G. Hinton, "Deep learning," *Nature,* vol. 521, no. 7553, pp. 436-444, 2015.

[22] L.-d. Wang, W. Zhou, Y. Xing, N. Liu, M. Movahedipour, and X.-g. Zhou, "A novel method based on convolutional neural networks for deriving standard 12-lead ECG from serial 3-lead ECG," *Frontiers of Information Technology & Electronic Engineering,* vol. 20, no. 3, pp. 405-413, 2019.

[23] T. Zebin, P. J. Scully, N. Peek, A. J. Casson, and K. B. Ozanyan, "Design and implementation of a convolutional neural network on an edge computing smartphone for human activity recognition," *IEEE Access,* vol. 7, pp. 133509-133520, 2019.

[24] B. Zhou, J. Yang, and Q. Li, "Smartphone-based activity recognition for indoor localization using a convolutional neural network," *Sensors,* vol. 19, no. 3, p. 621, 2019.

[25] T. M. Ghazal and G. Issa, "Alzheimer disease detection empowered with transfer learning," *Computers, Materials & Continua,* vol. 70, no. 3, pp. 5005-5019, 2022.

[26] M. Lotfollahi *et al.*, "Mapping single-cell data to reference atlases by transfer learning," *Nature Biotechnology,* vol. 40, no. 1, pp. 121-130, 2022.

[27] A. Saber, M. Sakr, O. M. Abo-Seida, A. Keshk, and H. Chen, "A novel deep-learning model for automatic detection and classification of breast cancer using the transfer-learning technique," *IEEE Access,* vol. 9, pp. 71194-71209, 2021.

[28] K. Weimann and T. O. Conrad, "Transfer learning for ECG classification," *Scientific reports,* vol. 11, no. 1, pp. 1-12, 2021.

[29] M. S. Ali, M. S. Miah, J. Haque, M. M. Rahman, and M. K. Islam, "An enhanced technique of skin cancer classification using deep convolutional neural network with transfer learning models," *Machine Learning with Applications,* vol. 5, p. 100036, 2021.

[30] S. Khandelwal and N. Wickström, "Evaluation of the performance of accelerometer-based gait event detection algorithms in different real-world scenarios using the MAREA gait database," *Gait & posture,* vol. 51, pp. 84-90, 2017.

[31] H. B. Kim *et al.*, "Wrist sensor-based tremor severity quantification in Parkinson's disease using convolutional neural network," *Computers in biology and medicine,* vol. 95, pp. 140-146, 2018.

[32] D.-H. Kang, Y.-J. Lee, J.-W. Lee, and J.-H. Lee, "A study on the sleeve-shaped platform of POF-based joint angle sensor for arm movement-monitoring clothing," *Science of Emotion and Sensibility,* vol. 14, no. 2, pp. 221-226, 2011.

[33] W. Huang, H. Zhang, X. Quan, and J. Wang, "A Two-level Dynamic Adaptive Network for Medical Image Fusion," *IEEE Transactions on Instrumentation and Measurement,* 2022.

[34] M. Bahrami and M. Forouzanfar, "Sleep apnea detection from single-lead ECG: a comprehensive analysis of machine learning and deep learning algorithms," *IEEE Transactions on Instrumentation and Measurement,* 2022.

[35] D. Mitra, H. Zanddizari, and S. Rajan, "Investigation of kronecker-based recovery of compressed ecg signal," *IEEE Transactions on Instrumentation and Measurement,* vol. 69, no. 6, pp. 3642-3653, 2019.

[36] A. Ravelomanantsoa, H. Rabah, and A. Rouane, "Simple and efficient compressed sensing encoder for wireless body area network," *IEEE Transactions on Instrumentation and Measurement,* vol. 63, no. 12, pp. 2973-2982, 2014.

[37] Q. Zhang, D. Arney, J. M. Goldman, E. M. Isselbacher, and A. A. Armoundas, "Design Implementation and Evaluation of a Mobile Continuous Blood Oxygen Saturation Monitoring System," *Sensors,* vol. 20, no. 22, p. 6581, 2020.

[38] D. Ayata, Y. Yaslan, and M. E. Kamasak, "Emotion based music recommendation system using wearable physiological sensors," *IEEE transactions on consumer electronics,* vol. 64, no. 2, pp. 196-203, 2018.

[39] B. Jiang, J. Yang, Z. Lv, and H. Song, "Wearable vision assistance system based on binocular sensors for visually impaired users," *IEEE Internet of Things Journal,* vol. 6, no. 2, pp. 1375-1383, 2018.

[40] C. Park, C. C. Took, and J.-K. Seong, "Machine learning in biomedical engineering," vol. 8, ed: Springer, 2018, pp. 1-3.

Kiirthanaa Gangadharan is a graduate student in Department of Electrical and Computer Engineering, Purdue University School of Engineering and Technology, Indianapolis, USA. Her research area includes smart health, deep learning, machine learning, transfer learning, rehabilitation, and wearable technologies.

Qingxue Zhang (Senior Member, IEEE) has over fifteen years' experience in both academia and industry, with his postdoc research at Harvard, products R&D in ICT, and Ph.D. research at University of Texas at Dallas. He started the faculty position at Purdue University School of Engineering & Technology, USA, in 2018. He is directing the Ubiquitous Intelligence Lab, with research interests including Deep Learning, IoT/Wearable, Edge Computing, and Brain-inspired Learning, targeting smart health, home, and world applications.

He is a recipient of the prestigious USA NSF CAREER Award. He serves as USA NSF/NIH/NIST Grant Review Panelists, IEEE workshop chair, AE for IEEE Access, AE for Consumer Electronics Magazine, and committee for multiple IEEE conferences. He received the Featured Journal Article Award in IEEE Access, the Best Paper Award in UEMCON2017, the Early-Career Travel Award in AHA2020, the Favorite Professor Award in 2019, and the Google Cloud Award in 2019. He is a member of the IEEE Instrumentation and Measurement Society, and a senior member of IEEE.